ISSN 0023-1584, Kinetics and Catalysis, 2007, Vol. 48, No. 5, pp. 728–734. © MAIK "Nauka/Interperiodica" (Russia), 2007.
Original Russian Text © P.G. Tsyrul'nikov, T.N. Afonasenko, S.V. Koshcheev, A.I. Boronin, 2007, published in Kinetika i Kataliz, 2007, Vol. 48, No. 5, pp. 778–784.

State of Palladium in Palladium–Aluminosilicate Catalysts As Studied by XPS and the Catalytic Activity of the Catalysts in the Deep Oxidation of Methane

P. G. Tsyrul'nikov[a], T. N. Afonasenko[a], S. V. Koshcheev[b], and A. I. Boronin[b]

[a] *Institute of Hydrocarbon Processing Problems, Siberian Branch, Russian Academy of Sciences, Omsk, Russia*
[b] *Boreskov Institute of Catalysis, Siberian Branch, Russian Academy of Sciences, Novosibirsk, 630090 Russia*
E-mail: tsyr@ihcp1.oscsbras.ru

Received August 14, 2006

Abstract—Palladium catalysts based on Siralox and AS aluminosilicate supports for the deep oxidation of methane were studied. With the use of XRD analysis, it was found that they were heterophase systems consisting of an amorphous aluminosilicate and γ-Al_2O_3 stabilized against agglomeration. It was found that the catalytic activity of palladium–aluminosilicate catalysts in the deep oxidation of methane at 500°C depended on the support precalcination temperature. X-ray photoelectron spectroscopy (XPS) was used to study the states of the AS-30 aluminosilicate support calcined at 600, 800, or 1000°C and palladium supported on it. It was found that the action of an acid impregnation solution of palladium nitrate on the aluminosilicate calcined at 800°C resulted in a structural rearrangement of the aluminosilicate surface. This rearrangement resulted in the stabilization of both palladium oxide and palladium metal particles at surface defects and the incorporation of these particles into the aluminosilicate after catalyst calcination. As a result, an anomalous decrease in catalytic activity was observed in aluminosilicate samples calcined at 800°C. According to XPS data, palladium in the catalyst was stabilized in the following three phases: metal (E_b(Pd $3d_{5/2}$) = 334.8 eV), oxide (E_b(Pd $3d_{5/2}$) = 336.8 eV), and "interaction" (E_b(Pd $3d_{5/2}$) = 335.8 eV) phases. The ratio between these phases depended on support and catalyst calcination temperatures. The interaction phase, which consisted of PdO_x clusters stabilized in the aluminosilicate structure, was responsible for the retention of activity after calcination at high temperatures (800°C). Based on an analysis of XPS data, it was hypothesized that palladium in the interaction phase occurred in a charged state with the formal charge on the Pd atom close to 1+ (δ+ phase).

DOI: 10.1134/S0023158407050187

INTRODUCTION

It is well known that palladium catalysts are commonly used in the reactions of CO oxidation and hydrocarbon afterburning; aluminum oxide [1] or zeolite [2–4] most frequently serves as supports in these catalysts. Note that only a few studies were devoted to palladium catalysts supported on amorphous aluminosilicates, although these supports exhibit a number of advantages. It is well known that the addition of SiO_2 to Al_2O_3 prevents phase transitions in aluminum oxide [5] and results in an increase in the specific surface area, which remains sufficiently large even after calcination at 1000°C (this is uncharacteristic of pure aluminum oxide). At the same time, the inner surface of these aluminosilicates is much more accessible to reactants than the surface of zeolite channels and cavities.

Thus, the aim of this work was to choose aluminosilicate supports for the development of active and thermally stable catalysts for deep methane oxidation and to characterize both the parent supports and palladium catalysts on these supports using physicochemical techniques. Because the thermal stability of catalysts mainly depends on the thermal stability of the supports, we used aluminosilicate supports whose specific surface area was >200 m^2/g even after calcination at 1000°C in order to develop supported palladium catalysts for the catalytic combustion of methane. X-ray photoelectron spectroscopy (XPS) was used as the main physicochemical technique for the characterization of supported palladium catalysts. The states of palladium on the surface of aluminosilicate supports subjected to various thermal treatments were characterized in detail with the use of this technique. The main purpose of XPS was to identify the specific palladium phase that is responsible for high activity after calcination at elevated temperatures.

EXPERIMENTAL

Supports. AS (fraction of 7–11 μm) and Siralox (25–90 μm) aluminosilicate supports from Condea and Sasol (Germany) were used in this study. Table 1 summarizes the compositions of these supports.

Specific surface area. The specific surface areas (S_{sp}) of samples were determined from the single-point adsorption of nitrogen with the use of a Sorpty 1750

Table 1. Concentrations of aluminum oxide and silicon oxide in AS and Siralox aluminosilicates

Component concentrations, %	Support			
	AS-5	AS-30	Siralox 5/320	Siralox 10/360
Al_2O_3	94.0	74.1	94.0	89.9
SiO_2	5.5	25.1	6.0	10.1

instrument (Carlo Erba, Italy) at $T = 77$ K and $P/P_s = 0.18$ with the relative error $\Delta = \pm 4\%$.

X-ray diffraction (XRD) analysis. The XRD analysis of the supports and catalysts was performed using a DRON-3 instrument (Russia) with monochromated CuK_α radiation and a β filter.

Preparation of palladium catalysts supported on aluminosilicates. The supports were precalcined in a muffle furnace at 600, 800, and 1000°C for 6 h and used for the preparation of catalysts with a palladium content of 2 wt %. Palladium was supported from a palladium nitrate solution, which was prepared by dissolving palladium black in nitric acid [6], onto a suspended support powder followed by evaporation in a water bath with stirring at regular intervals. After supporting the active component, the catalysts were dried at 120°C for 2 h and calcined at 800°C for 6 h.

Catalyst activity measurements. The activity of catalysts in the deep oxidation of methane was determined using a flow-circulation method in the kinetic region with a prepared catalyst fraction of size 0.4–0.8 mm. The reaction rate of methane oxidation at a given reaction mixture composition and a specified temperature was taken as a measure of catalytic activity. The reaction mixture of 0.5 vol % CH_4 in air was fed into the reactor whose temperature was 500°C. A small volume of the mixture leaving the reactor was used for chromatographic analysis to determine the amount of unreacted methane with a flame-ionization detector. Chromatographic analysis conditions: packed column with a Polysorb-1 sorbent; carrier-gas (nitrogen) flow rate, 30 ml/min; hydrogen flow rate, 30 ml/min; air flow rate, 300 ml/min.

The rate of reaction was calculated from conversion, the flow rate of the reaction mixture, and the weight of the catalyst:

$$w = \frac{S_0 - S_x}{S_x}\frac{V}{m_{\text{Cat}} \times 3.6}, \text{ cm}^3\ \text{g}^{-1}\text{s}^{-1},$$

where V is the feed rate of the reaction mixture, l/h; m is the catalyst weight, g; S_0 is the chromatographic peak area corresponding to the initial concentration of methane; S_x is the chromatographic peak area corresponding to the current concentration of methane at the reactor outlet at the point t_x in time.

Determination of the extent of dispersion of supported palladium. The extent of dispersion of supported palladium was determined using hydrogen–oxygen titration in accordance with a published procedure [7]. Before the determination, palladium catalysts were reduced with hydrogen at 500°C for 2 h.

XPS of the supports and catalysts. The XPS study of the supports and catalysts was performed on an ES 300 electron spectrometer (Kratos Analytical, the United Kingdom). The electron emission from a sample was performed using MgK_α soft X-ray radiation so that the mean free path of electrons (λ) was 20–30 Å depending on analytical lines. Thus, the analyzed thickness of the sample surface was equal to about 3λ, that is, 60–90 Å.

The samples were fixed in a holder using a vacuum-tight double-faced adhesive tape. The samples were pumped to $P = 10^{-7}$ mbar before spectroscopic measurements, and the vacuum in the course of measurements was no worse than 10^{-8} mbar. The main background gases were CO, CO_2, and H_2O.

The energy scale was calibrated using the Au $4f_{7/2}$ and Cu $2p_{3/2}$ binding energies, equal to 84.0 and 932.7 eV, respectively [7]. The experimental spectra were calibrated by shifting all of the detected photolines by a value that corresponded to an electrostatic shift of the C 1*s* peak, the true position of which was taken equal to 284.8 eV [8]. In the given samples, carbon served as an internal standard for lines corresponding to the binding energies of the other elements. The spectra were measured in the retarding-potential mode with a constant energy of electron transmission through a hemispherical analyzer.

The recording of lines with $HV = 25$ eV was used for the detailed analysis of the electronic states of catalyst components and the quantitative determination of the elemental composition. This ensured a high energy resolution of ~1.3 eV in terms of the full width at half maximum (fwhm) of the Ag $3d_{5/2}$ reference line. The spectroscopic data processing (calibration, integration, background correction, smoothing, the subtraction of X-ray satellites and ghost lines, deconvolution into individual components and doublets, etc.) was performed using the WinCalc software package, which was tested in various systems [9–11].

The chemical composition of sample surfaces was calculated using the ratio between integrated line intensities, which were precisely measured at the same analyzer pass energy with consideration for atomic sensitivity factors.

Table 2. Changes in the S_{sp} of supports after calcination

Support	S_{sp}, m^2/g		
	calcination temperature, °C		
	600	800	1000
Siralox 5/320	319	261	222
Siralox 10/360	371	294	235
AS-30	236	236	237
AS-5	203	210	205

RESULTS AND DISCUSSION

Study of the Thermal Stability of Supports

To evaluate the thermal stability, the supports were calcined at 600, 800, and 1000°C for 6 h. The thermal stability of aluminosilicates was judged from changes in their specific surface areas as the temperature was increased. Table 2 summarizes the results.

The experimental data suggest that aluminosilicates from the AS series exhibited the highest stability upon thermal treatment because the temperature action did not exert a noticeable effect on their specific surface areas. In the case of aluminosilicates from the Siralox series, an increase in the calcination temperature resulted in a decrease in the value of S_{sp}. However, even after calcination at 1000°C, the values of $S_{sp} \geq 200$ m^2/g were retained in all of the above supports.

In the course of the XRD analysis of all of the aluminosilicates calcined at 1000°C, only the phase of γ-Al_2O_3 was detected in the diffraction patterns; this is indicative of the stabilizing effect of silica on this phase. It is well known that 1000°C γ-Al_2O_3 changes to the θ-Al_2O_3 high-temperature phase at 1000°C. In this case, γ-Al_2O_3 exhibited coherent-scattering regions of size ~5 nm. The lattice parameter of γ-Al_2O_3 in the aluminosilicate was $a_0 = 79.3$ Å, that is, somewhat greater than $a_0 = 79.0$ Å for pure γ-Al_2O_3; this suggests the formation of a solid solution based on γ-Al_2O_3. Based on the experimental results, we can conclude that these supports are heterophase systems stable against temperature effects; these systems consist of an amorphous aluminosilicate phase and a stabilized γ-Al_2O_3 phase.

XPS Study of the Catalysts and Supports

For an XPS study, we used catalysts supported on AS-30 and the parent aluminosilicate. The survey photoelectron spectra of the AS-30 aluminosilicate and catalysts on its basis suggest that these spectra were fully typical of the entire series of test samples, and they mainly contained lines due to catalyst components. Impurities other than carbon were not detected.

The absolute concentrations of elements cannot be reliably determined from XPS data; however, the atomic ratios or overall compositions can be determined. In this work, we determined the atomic ratios of the elements with respect to aluminum. Data were calculated from the integral intensities of Al 2*p*, Si 2*p*, C 1*s*, O 1*s*, and Pd 3*d* lines with consideration for atomic sensitivity factors [8].

The O/Al ratio in the parent AS-30 support decreased as the temperature of precalcination was increased from 600 to 1000°C (Fig. 1). It is our opinion that this was due to an increase in the solubility of aluminum oxide, that is, an increase in the fraction of alumina as a constituent of the aluminosilicate because of the available free phase of γ-Al_2O_3. As a result, the O/Al ratio in the near-surface aluminosilicate layer also decreased because of the greater abundance of Al_2O_3, as compared with that of SiO_2. At the same time, S_{sp} in these samples remained at the same level regardless of the temperature of calcination (Table 1). The situation dramatically changed after supporting palladium on these supports.

Figures 1 and 2 indicate that the O/Al and Si/Al ratios noticeably increased after supporting palladium and calcining the catalysts. The increase of oxygen was due to a change in the Si/Al ratio in favor of silicon (SiO_2) rather than directly due to palladium compounds like PdO and $PdSiO_3$ because the concentration of Pd was relatively low.

Indeed, even if 2 wt % palladium formed a monolayer on the aluminosilicate surface, palladium would occupy ~10 m^2 (less than 5% of the specific surface

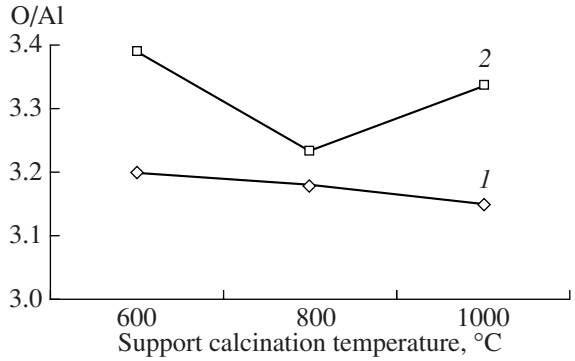

Fig. 1. O/Al ratios for the (*1*) AS-30 aluminosilicate and (*2*) 2% Pd/AS-30 catalyst.

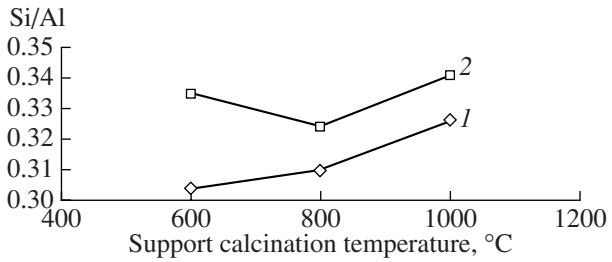

Fig. 2. Si/Al ratios for the (*1*) AS-30 aluminosilicate and (*2*) 2% Pd/AS-30 catalyst.

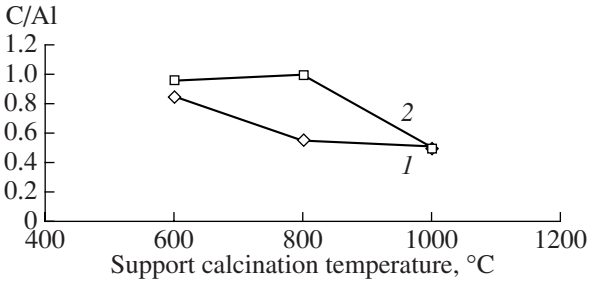

Fig. 3. C/Al ratios for the (*1*) AS-30 aluminosilicate and (*2*) 2% Pd/AS-30 catalyst.

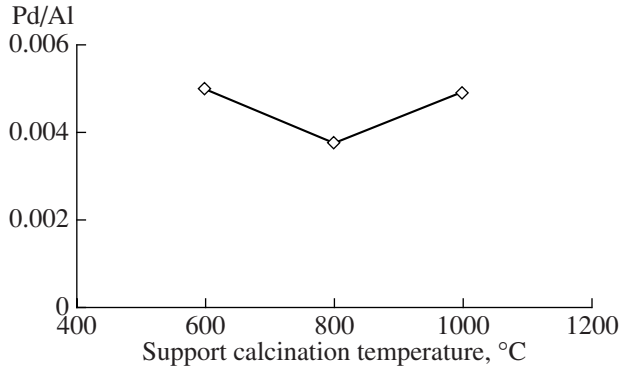

Fig. 4. Pd/Al ratio for the 2% Pd/AS-30 catalyst.

area of the aluminosilicate). Really, as found by hydrogen–oxygen titration, the dispersity (*D*) of supported palladium on AS-30 samples calcined at 600, 800, or 1000°C was equal to 15, 16, and 7%, respectively; this additionally decreased the surface area of supported Pd (PdO) to 1.5 and 0.7 m^2/g.

Nevertheless, the O/Al and Si/Al ratios dramatically increased after supporting palladium; a decrease in the relative concentration of Al in the surface layer was detected by XPS in all of the palladium-containing samples supported on AS-30. The possible reasons can be the following: Because an acid solution (pH ~ 1) of palladium nitrate with dispersed powder aluminosilicates, in particular, AS-30, was evaporated with stirring, a portion of the surface alumina constituent of aluminosilicates was leached with the formation of aluminum oxonitrates. It is most likely that these compounds were diffusion-transported to the surface of support grains where they underwent reprecipitation to form coarser particles of amorphous alumina in the course of drying and calcination. Indeed, Anan'in and Trokhimets [12] found that the amount of aluminum ions that passed to an acidic aqueous solution from a unit surface area of Al_2O_3 increased as the oxide calcination temperature was increased to 1120 K. By this is meant that the solubility of γ-Al_2O_3 in acidic solutions increased to a precalcination temperature of 850°C. We believe that this was due to a decrease of the protective hydroxyl surface coverage upon high-temperature dehydration. However, if an aluminosilicate containing the γ-Al_2O_3 phase was calcined at 1000°C before supporting palladium, the interaction of acidic impregnation solutions with the surface of the alumina phase decreased, probably because of the more intense dissolution of SiO_2 in alumina with the formation of a solid solution and a better crystallinity of γ-Al_2O_3 particles.

In our case, the Pd/AS-30 catalyst sample calcined at 800°C, which was prepared on the AS-30 support also precalcined at 800°C (Pd/AS-30-800), exhibited anomalously low Si/Al and O/Al ratios, as compared with the corresponding values for the samples of the above catalysts prepared on the AS-30 support calcined at 600 and 1000°C. In our opinion, the reason is a considerable rearrangement of the aluminosilicate surface structure under the action of acidic impregnation solutions, particularly in the case of the support calcined at 800°C. The subsequent thermal treatment of the catalyst sample resulted in many defects, which caused the insertion of carbon into the near-surface layer. Indeed, according to XPS data, this sample exhibited the greatest amount of carbon (Fig. 3); we believe that this carbon stabilized surface defects. The spectra of the Pd/AS-30-800 sample suggest that its surface underwent the strongest rearrangement to change its composition and hence exhibited the greatest structure imperfection. Typically, the support surface was more ordered upon catalyst formation on a support precalcined at 1000°C, so that the amount of carbon became much smaller. This can be explained by the weaker interaction of an acidic impregnation solution with the support calcined at 1000°C.

State of Palladium in Aluminosilicates

Figure 4 shows data on the relative surface concentrations of palladium (Pd/Al ratios). These data indicate that the average concentration of palladium was 0.5 at %; however, the Pd/AS-30-800 sample exhibited a somewhat lower value, probably because of a change in the above structural properties of the support surface.

Figure 5 shows the Pd 3*d* spectra of three test catalyst samples prepared on supports precalcined at 600, 800, and 1000°C. The spectra were calibrated using the C 1*s* line (see Experimental) and normalized with respect to the background of the Pd 3*d* line at lower binding energies. This was made in order to compare precisely Pd 3*d* line shapes with respect to each other. Indeed, as can be seen in Fig. 5, the Pd 3*d* line shapes varied from one sample to another. Because of this, we performed a background subtraction procedure and the curve fitting of the integral Pd 3*d* spectra into separate components. Figure 6 shows the results of this processing. All of the spectra were found complex and consisting of a few components. Thus, the Pd 3*d* spectrum of the 2% Pd/AS-30-600 sample was found to consist of a combination of three lines, which were characterized by the $3d_{5/2}$ component peak positions with E_b = 335.6, 336.8, and 338.6 eV. The component with E_b = 336.8 eV

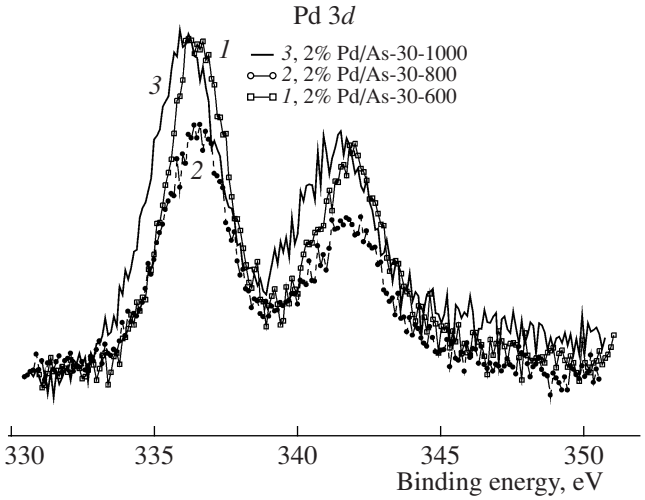

Fig. 5. Normalized and calibrated Pd 3*d* spectra of 2% Pd/AS-30 catalysts prepared on aluminosilicates calcined at various temperatures: (*1*) 600, (*2*) 800, and (*3*) 1000°C.

can be reliably attributed to the state of palladium in the PdO oxide phase in accordance with previously published data for the oxide phase [13–16]. In addition, we performed the oxidation of palladium foil with oxygen at high temperatures to the state of a continuous film of PdO and obtained a value of E_b(Pd $3d_{5/2}$) = 337.0 eV, which is practically equal to the value obtained by the spectroscopic treatment of the test supported catalysts.

The doublet at E_b(Pd $3d_{5/2}$) = 338.6 eV formally corresponds to the state Pd^{4+}; however, it is most likely that this spectrum component is a satellite line accompanying electron ionization from the Pd 3*d* level of palladium atoms in PdO particles. This conclusion is based on an analysis of both published spectroscopic data [7, 8, 13] and the experimental spectra of Pd metal and oxidized Pd foil, which exhibited satellite lines along with photolines [13]. According to Pilloy et al. [13], in the oxide phase, the most intense satellite is spaced at ~9 eV from the main line, whereas the satellite is spaced at ~6 eV in the palladium metal phase.

It is most likely that the peak at E_b = 334.8 eV in the Pd 3*d* spectra belongs to nanosized palladium particles. The binding energy 334.8 eV is close to the value of E_b for the state of palladium in the bulk metal phase (E_b = 335.2 eV) [7, 8]. Decreased values of E_b(Pd $3d_{5/2}$) are characteristic of the state of palladium atoms with a coordination number of <12, which is characteristic of palladium in the bulk metal. These states of palladium were detected on various faces of a single crystal of palladium [14, 15], where the coordination number was, on average, 6–9. The state of palladium atoms in disperse (nanosized) metal clusters is analogous to the state of these atoms on the surface of a single crystal. In these clusters, the state of palladium is also characterized by smaller coordination numbers and, correspondingly, values of E_b(Pd $3d_{5/2}$) lower than 335.2 eV.

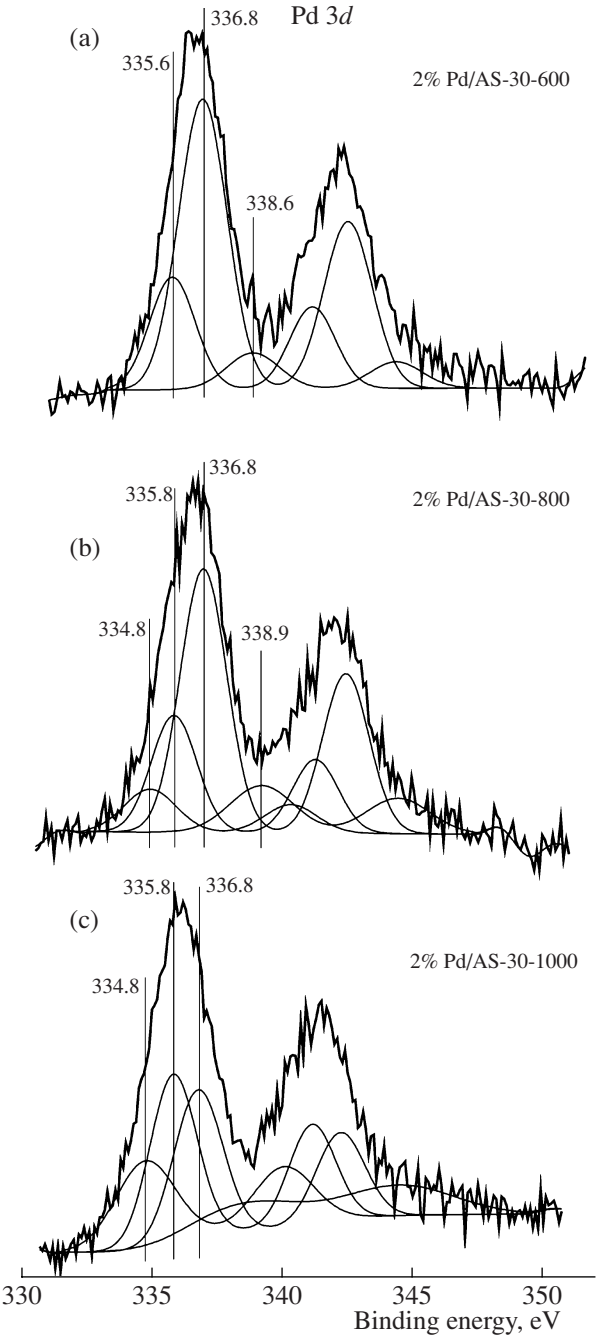

Fig. 6. Curve fitting of the Pd 3*d* spectra into components using Voight functions with consideration for Shirley background and instrumental resolution.

The appearance of a pronounced broad peak at E_b ~ 346 eV (Fig. 6c), which corresponds to the plasmon satellite of palladium metal, demonstrates that the peak with E_b(Pd $3d_{5/2}$) = 334.8 eV belongs to the state of palladium in metal clusters.

Finally, we dwell on the interpretation of a peak characterized by E_b(Pd $3d_{5/2}$) = 335.6–335.8 eV. Formally, this state of palladium can be attributed to Pd^+ ions. First, note that the contribution of this state of pal-

ladium to the total spectrum increased with the temperature of support precalcination and became predominant in the 2% Pd/AS-30-1000 catalyst, whereas the contribution of the component due to PdO particles considerably decreased. It is believed that this state of palladium resulted from heterophase aluminosilicate supports and the strong interaction of palladium oxide particles with the support, especially at interfaces between γ-Al_2O_3 crystals and amorphous aluminosilicate. In this case, an interaction phase was formed, in which palladium atoms or very small clusters were incorporated into the lattice of the support surface, most likely at extensive defects like steps and plane disruptions, which were concentrated at interfaces. These (metal or oxide) clusters cannot be large because the E_b of large clusters coincides with the value of E_b(Pd $3d_{5/2}$) = 335.2 eV (Pd metal) or 337.0 eV (PdO). The value of E_b(Pd $3d_{5/2}$) = 335.8 eV suggests a charged state of palladium particles in this interaction phase. The charged state of a cluster can be obtained as a consequence of either a strong interaction with the support at the cluster boundary or a strong polarizing effect of the matrix. Taking into account that the observed state of palladium was thermally stable, we believe that the charged palladium cluster was stabilized by the strong interaction at the boundary with the formation of chemical bonds through oxygen atoms to the support surface. Sohn et al. [16], who studied the state of palladium on the surface of SLMA hexaaluminate, observed the charge state of palladium $Pd^{\delta+}$ and obtained the value of E_b(Pd $3d_{5/2}$) = 335.8 eV. It was found that this state is also thermally stable up to T = 1200°C. As can be seen in Fig. 6, this state of palladium on aluminosilicate calcined at 1000°C before supporting palladium and then (with palladium) at 800°C became predominant. In terms of thermal stability, this state was much superior to the state of Pd in PdO clusters, which are thermodynamically unstable at 800°C.

Palladium stabilized as ions in extensive defects participated in the production of an intermediate interaction layer between the support and palladium metal clusters and bound the metal clusters to the support. In this case, the average positive charge $\delta+$ occurred at the palladium atom in a cluster. Evidently, this chemical interaction produced a stabilization effect on the active component at the sites of structural distortions of the support, which is responsible for the stability of metal clusters to agglomeration. In turn, in spite of the charged state, these clusters retained metallic character (the presence of Pd–Pd bonds), which was responsible for the retention of catalyst activity at high temperatures. Indeed, the palladium metal phase (Pd(0)) is inactive in deep oxidation reactions, whereas charged (oxidized) palladium particles, in which the Pd–Pd bond is retained, are active [17]. This explains the high activity of the palladium catalyst (calcined at 800°C) supported on AS-30, which was calcined at 1000°C before supporting palladium (Table 3).

Table 3. Activity* of 2.0 wt % PD/aluminosilicate catalysts in the reaction of deep methane oxidation at T = 500°C

Support	Support calcination temperature, °C		
	600	800	1000
Siralox 10/360	8.4	6.0	8.3
Siralox 5/320	8.6	6.7	8.7
AS-5	8.6	4.1	8.4
AS-30	5.5	3.7	7.9

Note: The catalyst calcination temperature was 800°C (6 h).
* Activity expressed as $w \times 10^{-2}$, cm^3 (g Cat)$^{-1}$ s^{-1}.

Catalytic Activity Testing

Table 3 summarizes the results of testing Pd/aluminosilicate catalysts in the reaction of deep methane oxidation.

As noted above, the activity of catalysts on supports calcined at 1000°C with a decreased dispersity of palladium (D = 7% for 2% Pd/AS-30-800) was retained because of the state of Pd with E_b(Pd $3d_{5/2}$) = 335.8 eV. Indeed, in these samples, the concentration of the active component as PdO particles was much lower and the concentration of $Pd^{\delta+}$ particles was higher than those in catalysts on supports calcined at lower temperatures.

It is likely that the metal state of palladium did not play a crucial role because no metal palladium particles were detected in the 2% Pd/AS-30-600 samples and the catalytic activity was equal to that of the 2% Pd/AS-30-1000 sample, in which a considerable portion of palladium was detected as metal particles. This is explained by the higher dispersity of PdO (16% on a reduced palladium basis) on the support initially calcined at 600°C, even though this sample with supported palladium was then calcined at 800°C.

An anomalous change in the activity of Pd/aluminosilicate catalysts on the supports precalcined at 800°C (before supporting palladium) in the reaction of methane oxidation was observed (Table 3). This anomaly can be traced in all of the test palladium catalysts based on heterophase aluminosilicate supports.

As follows from the above results of XPS studies, the occurrence of this "catalytic well" at 800°C is related to a structural rearrangement of the support in the course of thermal treatments. This structural rearrangement resulted in a decrease in the XPS signal intensities of Pd (Figs. 5, 6). As noted above, this decrease was due to the screening effect of photoemission, most likely because of the incorporation of palladium at the boundaries of aluminosilicate and aluminum oxide rather than the agglomeration of palladium.

CONCLUSIONS

In this work, it was demonstrated that Siralox and AS aluminosilicate supports retained S_{sp} of about

200 m^2/g after calcination at 1000°C. The temperature dependence of the states of the support and active component in the 2 wt % Pd/aluminosilicate catalysts was studied by XPS using the 2% Pd/AS-30 system as an example. It was found that calcination at 800°C resulted in a structural rearrangement in the aluminosilicate surface layer. This caused a noticeable decrease in the activity of the catalyst prepared with the use of the aluminosilicate calcined at 800°C in the reaction of deep methane oxidation, as compared with that of the catalyst samples on the supports precalcined at 600 and 1000°C. With the use of XPS, it was found that the state of the active component was determined by the following three phases: metal (E_b(Pd $3d_{5/2}$) = 334.8 eV), oxide (E_b(Pd $3d_{5/2}$) = 336.8 eV), and interaction (E_b(Pd $3d_{5/2}$) = 335.8 eV) phases. The ratio between the states of palladium in these phases depended on support and catalyst calcination temperatures. The interaction phase was responsible for the retention of activity after catalyst calcination at high temperatures (800°C). The relative amount of this phase was greater on a less disperse catalyst whose support was calcined at 1000°C. Based on an analysis of XPS data, it was hypothesized that palladium particles in the interaction phase occurred in a charged state with the formal charge 1+ on the Pd atom (δ^+ phase).

REFERENCES

1. Al'tshuler, M.A., Svintsova, L.G., Shimanovskaya, V.V., and Sklyar, V.T., *Dokl. Akad. Nauk Ukr. SSR, Ser. C*, 1981, no. 12, p. 37.
2. Slovetskaya, K.I. and Kustov, L.M., *Izv. Akad. Nauk, Ser. Khim.*, 2003, no. 9, p. 1832.
3. Radkevich, V.Z., Savchits, M.F., and Egiazarov, Yu.G., *Zh. Prikl. Khim.*, 1997, vol. 70, no. 5, p. 797 [*Russ. J. Appl. Chem.* (Engl. Transl.), vol. 70, no. 5, p. 759].
4. Tagiev, D.B. and Minachev, Kh.M., *Usp. Khim.*, 1981, vol. 40, no. 11, p. 1929.
5. Ismagilov, Z.R., Shkrabina, R.A., and Koryabkina, N.A., in *Alyumooksidnye nositeli: Proizvodstvo, svoistva i primenenie v kataliticheskikh protsessakh zashchity okruzhayushchei sredy* (Alumina Supports: Production, Properties, and Use in Catalytic Processes for Environmental Protection), Novosibirsk, 1998, issue 50, p. 56.
6. Chzhu, D.P., Tsyrul'nikov, P.G., Kryukova, G.N., Borbat, V.F., Kudrya, E.N., Smolikov, M.D., and Bubnov, A.V., *Kinet. Katal.*, 2004, vol. 45, no. 3, p. 432 [*Kinet. Catal.* (Engl. Transl.), vol. 45, no. 3, p. 406].
7. *Practical Surface Analysis by Auger and X-ray Photoelectron Spectroscopy*, Briggs, D. and Seah, M., Eds., Chichester: Wiley, 1983.
8. Moulder, J.F., Stickle, W.F., Sobol, P.E., and Bomben, K.D., *Handbook of X-ray Photoelectron Spectroscopy*, Eden Prairie, Minn.: Perkin-Elmer, 1992.
9. Slavinskaya, E.M., Chesalov, Yu.A., Boronin, A.I., Polukhina, I.A., and Noskov, A.S., *Kinet. Katal.*, 2005, vol. 46, no. 4, p. 590 [*Kinet. Catal.* (Engl. Transl.), vol. 46, no. 4, p. 555].
10. Titkov, A.I., Salanov, A.N., Koscheev, S.V., and Boronin, A.I., *React. Kinet. Catal. Lett.*, 2005, vol. 86, no. 2, p. 371.
11. Knyazev, A.S., Magaev, O.V., Vodyankina, O.V., Titkov, A.I., Salanov, A.N., Koshcheev, S.V., and Boronin, A.I., *Kinet. Katal.*, 2005, vol. 46, no. 1, p. 151 [*Kinet. Catal.* (Engl. Transl.), vol. 46, no. 1, p. 144].
12. Anan'in, V.N. and Trokhimets, A.I., in *Tezisy dokladov Vsesoyuznogo soveshchaniya "Nauchnye osnovy prigotovleniya katalizatorov"* (Proc. All-Union Conf. on the Scientific Foundations of Catalyst Preparation), Novosibirsk, 1983, p. 102.
13. Pilloy, Th., Zimmermann, R., Steiner, P., and Hufner, S., *J. Phys.: Condens. Matter*, 1997, vol. 9, p. 3987.
14. Leisenberger, F.P., Koller, G., Sock, M., Surnev, S., Ramsey, M.G., Netzer, F.P., Klotzer, B., and Hayek, K., *Surf. Sci.*, 2000, vol. 445, p. 380.
15. Todorova, M., Lundgren, E., Blum, V., Mikkelsen, A., Gray, S., Gustafson, J., Borg, M., Rogal, J., Reuter, K., Andersen, J.N., and Scheffle, M., *Surf. Sci.*, 2003, vol. 541, p. 101.
16. Sohn, Y.M., Kang, S.K., and Woo, S.I., *J. Mol. Catal. A: Chem.*, 2002, vol. 186, p. 135.
17. Kochubei, D.I., Starostina, T.G., Tsyrul'nikov, P.G., Popovskii, V.V., and Zamaraev, K.I., in *Tezisy dokladov IV Vsesoyuznoi konferentsii po mekhanizmu kataliticheskikh reaktsii* (Proc. IV Al-Union Conf. on Mechanisms of Catalytic Reactions), Moscow, 1986, vol. 2, p. 160.